# CLUSTERING CAUSAL ADDITIVE NOISE MODELS

#### A PREPRINT

### Vahid Partovi Nia

Huawei Noah's Ark Lab Montreal Research Centre vahid.partovinia@huawei.com

#### Xinlin Li

Huawei Noah's Ark Lab Montreal Research Centre xinlin.li1@huawei.com

### **Masoud Asgharian**

Department of Mathematics and Statistics McGill University

#### Shoubo Hu

Department of Computer Science and Engineering Chinese University of Hong Kong shoubo.hu@gmail.com

#### **Zhitang Chen**

Huawei Noah's Ark Lab Hong Kong Science Park chenzhitang2@huawei.com

#### Yanhui Geng

Huawei Noah's Ark Lab Montreal Research Centre geng.yanhui@huawei.com

October 27, 2021

## **ABSTRACT**

Additive noise models are commonly used to infer the causal direction for a given set of observed data. Most causal models assume a single homogeneous population. However, observations may be collected under different conditions in practice. Such data often require models that can accommodate possible heterogeneity caused by different conditions under which data have been collected. We propose a clustering algorithm inspired by the k-means algorithm, but with unknown k. Using the proposed algorithm, both the labels and the number of components are estimated from the collected data. The estimated labels are used to adjust the causal direction test statistic. The adjustment significantly improves the performance of the test statistic in identifying the correct causal direction.

**Keywords** additive noise model  $\cdot$  causal inference  $\cdot$  clustering  $\cdot$  k-means.

### 1 Introduction

Causal inference is one of the most fundamental concepts in learning. It is essentially learning how to connect the dots. To learn the *cause-and-effect* relationship between two factors using a random sample, we impose certain structures on the data generating process. One can infer which factor plays the role of *cause* and which one plays the role of *effect*. Univariate variables (factors) are denoted by small letters, e.g. x, vectors by bold small letter, e.g. x, while matrices by capital bold letter, e.g. x. We borrow the notation style of linear models, and denote random variables and their realizations both by small letters.

Understanding the data generating mechanism has been the main theme in causal inference. The causal direction between two random variables x and y is inferred using observed data from the random pair (x, y). The problem of

causal inference can be written simply as distribution decomposition. Assume  $(x,y) \sim p(x,y)$  follow a complex joint distribution. Causal inference looks for evidence in the observed data to prefer a certain conditional decomposition, either  $p(x,y) = p(y \mid x)p(x)$  or  $p(x,y) = p(x \mid y)p(y)$ . In the former decomposition x causes y or  $x \to y$  and in the latter decomposition y causes x or  $y \to x$ . In theory, both decomposition are valid and therefore causal inference without further assumptions is ill-defined and *unidentifiable*. Under more structural assumption such as the Additive Noise Model (ANM) the decomposition direction becomes *identifiable*, and observed data can be used to judge about the *cause-and-effect* relationship.

The additive noise model [4] represents the effect as a function of the cause with an additive independent noise  $y=f(x)+\varepsilon$ , in which  $f(\cdot)$  is a nonlinear deterministic smooth function that does not depend on x, and  $\varepsilon\sim p(\varepsilon)$  is an independent noise. There is no model of the form  $x=g(y)+\varepsilon$  that admits an ANM in the anti-causal direction [4] (unless  $g(\cdot)$  depend on  $\varepsilon,y$ , or both), i.e. the causal direction is identifiable from the anti-causal direction under ANM assumptions.

Most causal inference approaches assume a single causal model for the observed data, for instance [11], [13], and [6]. Due to the unknown data generation process and variability in data source, sampling scheme, sampling conditions, etc there is no single model guarantee in practice. Thus, focusing on a single causal model needs justifiable evidence, or at least requires a second thought. When observations are generated from a non-homogeneous population that is comprised of several homogeneous sub-populations, the number of homogeneous sub-populations affects the causal direction test statistic performance to a great extent. This calls for adjustment of the current causal inference methodology for many practical applications. Figure 1 provides a visual intuition, where the identified number of sub-populations heavily depends on the range within which x is observed. If x is observed about 0.7, a single component emerges. However, observing x about 0.5 or 1.0 changes the number of observed components to 2 or 3 respectively.

In many applications, data are combined from several different sources. Common causal models are more suitable for data of homogeneous nature. Naive use of the existing clustering algorithms can lead to misleading results as far as establishing causation is concerned. The existing clustering methods focus on observed data rather than the inherent functional process, so requires a proper adaptation for causal models.

Recently, [8] and [5] proposed inferring the causal direction on ANMs for discrete and continuous variables respectively. Here we focus on continuous variables. [5] proposed k-means on causal parameters and used a predetermined number of sub-populations to overcome data heterogeneity. They have not, however, used this information to correct the causal direction test statistic. It is evident that the clustering phase is unjustifiable if it does not help inferring the causal direction. Our work extends [5] on two directions: i) provide a clustering method with imprecise number of cluster components. ii) uses the clustering information to adjust the test statistic and reexamine the causal direction using clustering labels. Our codes are available at http://github.com/gituser/

We use a model in which the causal direction of the mixture of ANMs is identifiable, and we adopt Partially Observable Gaussian Process Model for model estimation [7].

### 2 Cluster additive noise model

Cluster additive noise model (CAN) is performed by fitting several models of the same causal direction [5]. We begin with model and estimation preliminaries.

For a given cluster the associated additive model is estimated, but in practice cluster labels are missing. Labels needs to be estimated either mutually or after parameter estimation. Following [5] we propose the latter approach which is computationally less demanding.

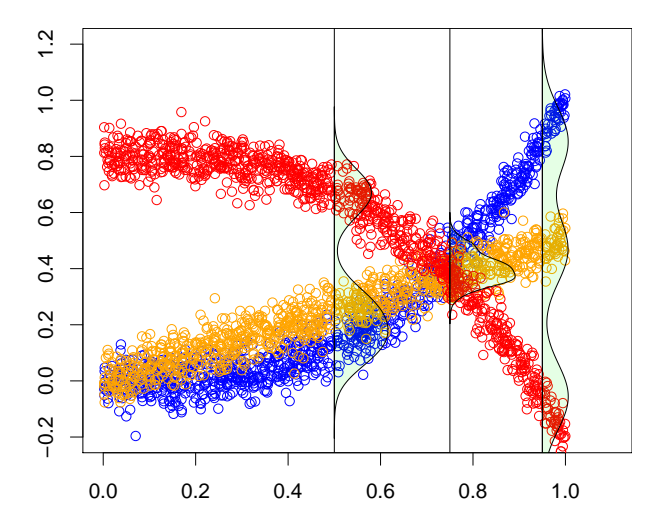


Figure 1: Illustration of from three clusters,  $y=x^3+\varepsilon$  (blue),  $y=0.5x+\varepsilon$  (orange),  $y=0.8-x^3+\varepsilon$  (red). The causal model imposes a different number of observed components depending on observed x, calling for a clustering with flexible component size.

**Definition 1** A cluster additive noise model is a set of causal models of the same causal direction between two continuous random variables x and y

$$y = f(x; \theta_c) + \varepsilon, \tag{1}$$

where x denotes the cause, y denotes the effect, f is a smooth function parametrized by nonlinearity parameters  $\theta_c$ , and  $\varepsilon \perp \!\!\! \perp x$  is the statistical noise.

The difference between traditional causal models and cluster causal model is the way that causal parameters  $\theta$  are treated. The nonlinearity parameter  $\theta_c$  is drawn randomly from a probabilistic model independently. In other words, a set of independent generating mechanisms is assumed for each sub-population through  $\theta_c$ . Our approach formulation is slightly different from that of [5], and assumes the causal parameters  $\theta_c$  are not drawn from a fixed set, but generated from an independent Gaussian distribution. Although this modification seems minor, it plays a major role in attaching the causal model to the clustering algorithm and allows to aggregate the causal test statistic through the cluster independence assumption. The model is also inspired by commonly encountered situations where the data generating process may be different, due to the influence of uncontrollable factors, from one independent trial to another. The data generating mechanism is depicted in Figure 2.

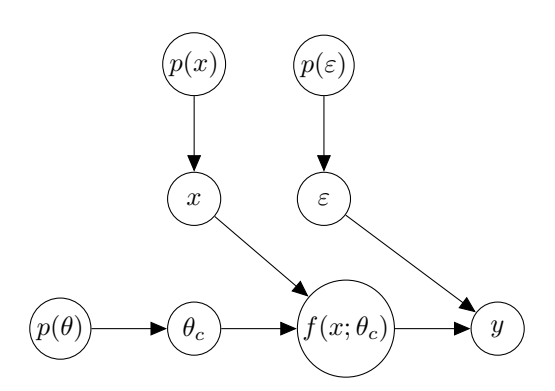


Figure 2: The generative process of a cluster additive noise model.

We assume if  $x \to y$ , the distribution of x and the function f mapping x to y are independent [6]. In a CAN, we interpret the independence between the cause and mechanism only through  $\theta_c$  that captures all properties of the mapping f, while  $\theta_c$  is independent of the cause x. We assume the model is identifiable, i.e. if  $x \to y$ , there is no backward additive noise model  $x = g(y; \nu_c) + \varepsilon$  that satisfies  $y \perp \!\!\! \perp \nu_c$ , see [5, Theorem 1]. In other words, if x is independent of  $\theta_c$  in the causal direction, it is likely that y and  $v_c$  are dependent in the anti-causal direction.

First we estimate the model parameters for each subject  $\theta_i, i=1,\ldots,n$ , and second we cluster  $\theta_i$  while the number of clusters k is imprecise. This maps  $\theta_i$  to  $\theta_c, c=1,\ldots,k$  while k varies  $K-\Delta \leq k \leq K+\Delta$  for a given  $\Delta$ .

We start the estimation process by projecting a set of centred n dimensional data  $\mathbf{x} = [x_1, \dots, x_n]^\top$  as the observed cause, and  $\mathbf{y} = [y_1, \dots, y_n]^\top$ , as the observed effect onto d hidden dimensions. The projection problem is formalized as the maximization of a Gaussian log-likelihood

$$\mathcal{L}(\mathbf{K}) = -\frac{dn}{2}\log(2\pi) - \frac{d}{2}\log|\mathbf{K}| - \frac{1}{2}\operatorname{tr}\left(\mathbf{K}^{-1}\mathbf{y}\mathbf{y}^{\top}\right),\,$$

where **K** is the covariance matrix  $\mathbf{K} = \boldsymbol{\phi} \boldsymbol{\phi}^{\top} + \boldsymbol{\beta}^{-1} \mathbf{I}$ ,  $\boldsymbol{\beta}$  is a positive scale, **I** is the identity matrix. The canonical nonlinear feature map  $\boldsymbol{\phi} = [\phi(x_1), \dots, \phi(x_n)]^{\top}$  is computed using the kernel trick.

The latent variable  $\theta_i$  is brought in the additive noise model through a concatenated latent predictor  $\tilde{\mathbf{x}}_i^{\top} = [x_i, \theta_i]$  and the Hilbert space is re-defined based on the new vector  $\tilde{\mathbf{x}}_i$ . Therefore, the latent parameters are estimated by maximizing the Gaussian log-likelihood

$$\mathcal{L}(\boldsymbol{\theta}) = -\frac{(d+1)n}{2}\log(2\pi) - \frac{d+1}{2}\log|\tilde{\mathbf{K}}| - \frac{1}{2}\operatorname{tr}\left(\tilde{\mathbf{K}}^{-1}\mathbf{y}\mathbf{y}^{\top}\right),\tag{2}$$

where  $\boldsymbol{\theta}$  is the vector composed of  $\theta_i$ 's,  $\tilde{\mathbf{K}} = \tilde{\boldsymbol{\Phi}} \tilde{\boldsymbol{\Phi}}^{\top}$ , and  $\tilde{\boldsymbol{\Phi}}_{n \times (d+1)} = [\phi(\tilde{\mathbf{x}}_1), \dots, \phi(\tilde{\mathbf{x}}_N)]$ . The parameter vector  $\boldsymbol{\theta}$  appears in  $\tilde{\mathbf{K}}$  through  $\tilde{\mathbf{x}}$ . In our developments we focus on univariate  $\theta_i$ , but the methodology is general and is valid for multivariate projection as well. This approach re-formalizes the additive model  $y = f(x, \theta) + \varepsilon$  in terms of the augmented variable  $y = f(\tilde{\mathbf{x}}) + \varepsilon$ . However, it is still the log-likelihood of an ill-defined CAN model, because x and  $\theta$  should be independent.

Hilbert-Schmidt independence criterion (HSIC) measures the dependence between observations of a pair of random variables through projecting them onto the reproducing kernel Hilbert space. The empirical HSIC is

$$HSIC = \frac{1}{n^2} \operatorname{tr}(\mathbf{KHLH}), \tag{3}$$

where **K** is kernel elements of  $x, k(x_i, x_{i'})$ , **L** is the kernel elements of  $y, l(y_i, y_{i'})$ ,  $\mathbf{H} = \mathbf{I} - \frac{1}{n} \mathbf{1} \mathbf{1}^{\top}$  and **1** is the unit vector of size n.

The independence between x and  $\theta$  is encouraged by adding HSIC as a regularizer to the log-likelihood term through the regularization constant  $\lambda > 0$ 

$$\mathcal{J}(\boldsymbol{\theta}) = \mathcal{L}(\boldsymbol{\theta}) - \lambda \log \mathrm{HSIC}(\boldsymbol{\theta}). \tag{4}$$

Causal parameters are estimated by  $\hat{\Theta} = \arg \max \mathcal{J}(\Theta)$  using scaled conjugate gradient maximization [5].

## 3 Clustering Method

We adopt the *product partition* model [3] for clustering causal observations, i.e.

$$f(\mathbf{x}, \mathbf{y} \mid \boldsymbol{\theta}, \mathbf{z}) = \prod_{c=1}^{k} \prod_{\{i \mid z_i = c\}} f(x_i, y_i \mid \theta_i)$$
 (5)

The clustering mechanism adds an unobserved label  $z_i$  to each observation, i.e.  $(x_i, y_i, z_i)$  or equivalently  $(\theta_i, z_i)$  in which  $z_i \in \{1, 2, \dots, k\}$  is the label and k is the uncertain number of sub-populations. The clustering methods relies on  $\theta_i \in \mathbb{R}$  which is the key to distinguish between different generating mechanisms. Note that for an identifiable mapping  $f_{\theta}$ , one can directly cluster generating mechanism only through clustering  $\theta_i$ 's.

Therefore,  $\theta_c$  in (5) is equivalent to the pair  $(\theta_i, z_i = c)$ . A practical causal cluster model should uncover the unknown sub-populations k as well as the unobserved label  $z_i$ . Therefore, we focus on devising an algorithm that allows for clustering  $\theta_i$  with a flexible component size  $k = \max(z_i) \in \{K - \Delta, \dots, K + \Delta\}$ , given positive integers K and K. The algorithm looks like a simple extension of K-means, but the inspiration comes from a probabilistic clustering that satisfies certain conditions to guarantee convergence. At the end we propose a deterministic variant that resembles K-means because it is straight-froward to implement and intuitive to understand.

### 3.1 Probabilistic Clustering

We first re-formalize probabilistic clustering model through Bayesian regression and derive the clustering algorithm using this model. This viewpoint allows us use the marginal posterior as an estimation tool for the cluster component size.

Assume the following Bayesian regression for the latent parameters

$$\theta \mid \boldsymbol{\mu} \sim \mathcal{N}(\mathbf{Z}\boldsymbol{\mu}, \sigma^2 \mathbf{I})$$

$$\boldsymbol{\mu} \sim \mathcal{N}(\bar{\boldsymbol{\theta}}, \kappa(\tau \sigma)^2 \mathbf{I}), \tag{6}$$

where  $\sigma^2$  is the common within-cluster variance,  $\tau^2$  is the between-cluster to within-cluster variance ratio, and  $\bar{\theta} = [\bar{\theta}_1, \dots, \bar{\theta}_k]$  is the vector of the cluster averages. The over-dispersion parameter  $\kappa > 1$  controls the prior information, i.e. a large  $\kappa$  value gives a flat prior with minimal prior information about the parameters. This model is a sort of *empirical Bayes* in which the data statistic is utilized to parameterize the prior.

The binary design matrix  $\mathbf{Z}_{N \times k}$  and the label vector  $\mathbf{z}$  are closely related. For instance in a two-population problem, the label  $\mathbf{z} = [1, 1, 2, 2, 2]$ , is equivalent to

problem, the label 
$$\mathbf{z} = [1,1,2,2,2]$$
, is equivalent to  $\mathbf{Z}^{\top} = \begin{bmatrix} 1 & 1 & 0 & 0 & 0 \\ 0 & 0 & 1 & 1 & 1 \end{bmatrix}$ , and  $\boldsymbol{\mu}^{\top} = [\mu_1,\mu_2]$ . Defining labels in terms of the matrix  $\mathbf{Z}$  reformulates clustering as

labels in terms of the matrix  $\mathbf{Z}$  reformulates clustering as the estimation of an optimal binary *design matrix*  $\mathbf{Z}$  in linear regression through maximizing

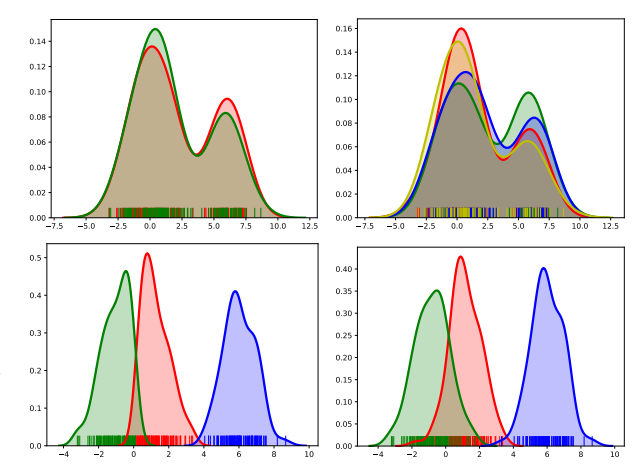


Figure 3: Simulated parameter  $\theta$ , before and after applying our clustering algorithm. Top panel: initialized labels with  $K=3, \Delta=1$ , i.e.  $k=K-\Delta$  (left), and  $k=K+\Delta$  (right). Bottom panel: the algorithm finds the correct cluster component size, converged labels (left) versus true labels (right).

$$\ell(\boldsymbol{\theta} \mid \mathbf{z}) = \log \int \cdots \int p(\boldsymbol{\theta} \mid \boldsymbol{\mu}, \mathbf{Z}) f(\boldsymbol{\mu} \mid \mathbf{Z}) d\boldsymbol{\mu}., \tag{7}$$

in which **Z** is an orthogonal binary matrix.

When  $\sigma \to 0$ , the Gaussian distribution converges to a degenerate distribution and our proposed algorithm becomes essentially the k-means algorithm for a given k. The probabilistic version (7), however, allows us estimate k and hence handle clustering with flexible components.

### 3.2 Clustering with Flexible Components

We propose to maximize  $p(\mathbf{z} \mid \boldsymbol{\theta}) \propto \exp\{\ell(\mathbf{z} \mid \boldsymbol{\theta})\}p(\mathbf{z})$  or simply  $\exp\{\ell(\boldsymbol{\theta} \mid \mathbf{z})\}$  for constant prior  $p(\mathbf{z})$ . Sampling from  $p(\mathbf{z} \mid \boldsymbol{\theta})$  and maximizing  $\ell(\mathbf{z} \mid \boldsymbol{\theta})$  coincide for a small temperature  $\sigma \to 0$ .

Estimating the normalizing constant of  $p(\mathbf{z} \mid \boldsymbol{\theta})$  for an unknown k is computationally expensive, while for a given k this normalizing constant is simply the sum over the discrete moves  $\sum_{c=1}^k p(z_i = c \mid \mathbf{z}_{-i}, \boldsymbol{\theta})$  in which  $z_i$  is the label of subject i, and  $\mathbf{z}_{-i}$  is all labels except i. This observation suggests several predetermined number of clusters within a reasonable range, say  $k \in \{K - \Delta, \dots, K + \Delta\}$ , where the normalizing constant can be computed effectively at each sampling iteration. We propose to break the clustering algorithm into two steps: i) sample from groupings for a given k, ii) move between different cluster component size k proportional to the marginal  $p(\mathbf{z} \mid \boldsymbol{\theta}, k)$ . Conditioning on k in i) fixes the dimension (7) and avoids trans-dimensional Markov chain sampler implementation.

	K		50			100	
	K	5	50 10	15	5	10	15
au							
5		1.5	3.3	4.0	1.6	3.1	4.0
10		0.5	2.8	4.0	0.7	2.8	4.0
50		0.0	1.0	2.6	0.0	3.1 2.8 1.0	2.6

Table 1: The vector  $\boldsymbol{\theta}$  simulated from (6) with  $\sigma=1,\kappa=1$ . Absolute bias  $|\hat{k}-K|$  averaged over 100 simulated data is reported, the smaller value is the better, and the random error is  $\pm 0.2$ . The data are clustered with  $k=K\pm 4$ .

A block Gibbs sampler of the full posterior  $(\mathbf{z}, \boldsymbol{\mu}) \sim p(\mathbf{z}, \boldsymbol{\mu} \mid \boldsymbol{\theta})$ , suggests to sample from  $p(\mathbf{z} \mid \boldsymbol{\mu}, \boldsymbol{\theta})$  and then from  $p(\boldsymbol{\mu} \mid \mathbf{z}, \boldsymbol{\theta})$ . Samples from the auxiliary variables  $\boldsymbol{\mu}$  are ignored and only  $\mathbf{z}$  is tracked, i.e.  $\mathbf{z} \sim p(\mathbf{z} \mid \boldsymbol{\theta})$ . Still jumping between samplers with different number of clusters k requires evaluation of the multivariate integral (7) which Theorem 1 resolves.

**Theorem 1** The log likelihood (7) can be simplified to

$$\ell(\mathbf{z} \mid \boldsymbol{\theta}, k) = -\frac{n}{2} \log 2\pi\sigma^2 - \frac{1}{2\sigma^2} \sum_{c=1}^{k} \sum_{\{i \mid z_i = c\}} (\theta_i - \bar{\theta}_c)^2 - \frac{1}{2} \sum_{c=1}^{k} \log(\kappa \tau^2 n_c + 1).$$
 (8)

where  $n_c$  is the size of the cth cluster and  $n = \sum_{c=1}^k n_c$ . This simplified log likelihood can be used to jump between models with a varying component k. Suppose the parameter vector  $\theta$  is given after maximizing (4). We suggest the following clustering method

- 1. Initialization: Set  $K, \Delta, \kappa$ , initialize **z**, compute  $n_c, \tau^2, \sigma^2$ .
- 2. Run  $2\Delta + 1$  clustering chains in parallel  $k \in \{K \Delta, \dots, K + \Delta\}$
- 3. For each chain of size k
  - 3.1) centre update:  $\mu_c = \bar{\theta}_c$
  - 3.2) label update:  $z_i = \arg\min_c |\theta_i \mu_c|$ .
- 4. Within-cluster variance computation:

$$\sigma^{2} = \frac{1}{N} \sum_{c=1}^{k} \sum_{\{i | z_{i} = c\}}^{n_{c}} (\theta_{i} - \bar{\theta}_{c})^{2}.$$

5. Between-to-within variance ratio computation:

$$\tau^2 = \frac{1}{k\sigma^2} \sum_{c=1}^k (\bar{\theta}_c - \bar{\theta})^2$$

6. Component size estimation:  $\hat{k} = \arg \max_{k} \ell(\mathbf{z} \mid \boldsymbol{\theta}, k)$ .

We iterate between 3.1 and 3.2 until convergence and ultimately report the labels  $\mathbf{z}$  with k that maximize  $\ell(\mathbf{z} \mid \boldsymbol{\theta}, k)$ . The clustering algorithm resembles the k-means to a great extend and only adds few more steps to estimates the cluster component size using the marginal log likelihood (7). The computational complexity of the clustering algorithm is  $\mathcal{O}(\Delta NK)$ . Figure 3 shows synthetic  $\boldsymbol{\theta}$  generated from 3 clusters, and the algorithm uncovers the true number of clusters.

**Theorem 2** The proposed probabilistic algorithm for clustering with the following steps converges to  $p(\mathbf{z} \mid \boldsymbol{\theta})$  for given  $\sigma^2$  and  $\tau^2$ 

- i) cluster centre update: sample from a Gaussian distribution with mean  $\bar{\theta}_c(1+\frac{1}{n_c\kappa\tau^2})^{-1}$  and variance  $\sigma^2(n_c+\frac{1}{\kappa\tau^2})^{-1}$ .
- ii) cluster label update: sample from Multinomial distribution with probabilities proportional to  $\phi\left(\frac{\theta_i-\mu_c}{\sigma}\right)$  in which  $\phi(\cdot)$  is a standard Gaussian density.
- iii) cluster component update: sample from Multinomial distribution with probabilities proportional to  $\exp\{\ell(\mathbf{z}\mid\boldsymbol{\theta},k)\}$ .

See the Appendix for the proof.

Next, we explore the efficiency of cluster component estimation in a brief simulation study. We simulate 100 random data, each composed of 5,10,15 balanced clusters generated from (6). Table 1 confirms that the estimation improves as data become more separable, i.e. as  $\tau$  increases. The estimation quality, however, remains relatively intact as the number of observations per clusters,  $n_c, c=1,2,\cdots,K$ , increases. The estimation becomes more difficult as K, the number of components, increases for a fixed separation parameter  $\tau$ .

## 4 Test Statistic Adjustment

In causal models HSIC is used to draw conclusions about the causal direction. This test statistic is, however, designed for a homogeneous single population sample and is highly sensitive to departure from this assumption. Theorem 3 presents the asymptotic distribution of the aggregated empirical HSIC using which inference about the causal direction in a heterogeneous case can be made.

**Theorem 3** Define  $\mathrm{HSIC}_c = \frac{1}{n_c^2}\operatorname{tr}(\mathbf{K}_c\mathbf{H}_c\mathbf{L}_c\mathbf{H}_c)$  to be the cluster-specific empirical HSIC statistic. The aggregated test statistic  $t = \sum_{c=1}^k n_c \mathrm{HSIC}_c$  converges in distribution to  $\sum_{l=1}^{\infty} \lambda_l z_l^2$ , where  $z_l$ ,  $l = 1, 2, \cdots$  are independent standard Gaussian random variables and  $\lambda_l$   $l = 1, 2, \cdots$  are non-negative constants.

The proof is given in the Appendix.

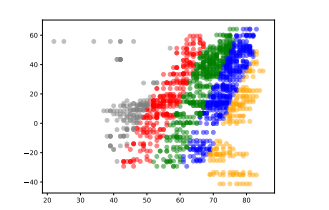
The result of Theorem 3 is aligned with that of [2] given for the homogeneous case. The aggregated test statistic is used to judge the causal direction.

The theoretical quantile of the test statistic t can be calculated using the the Gamma basis [12]  $\alpha = \frac{\mu^2}{\sigma^2}$  and  $\beta = \frac{\sigma^2}{\mu}$  with  $\mu = \sum_{c=1}^k n_c \mu_c$ ,  $\sigma^2 = \sum_{c=1}^k n_c^2 \sigma_c^2$ , in which  $\mu_c$  and  $\sigma_c^2$  are the cluster-specific theoretical HSIC mean and variance.

## 5 Application

Tüebingen cause-effect pairs [9] is a well-known benchmark in the context of causal direction detection  $^1$ . The database include 41 data sets arranged in 108 pairs (x,y) with a known causal direction identified for each pair, either  $x \to y$  or  $y \to x$ .

First we explore the effect of number of clusters on the test statistic for the UN life expectancy data by concatenating pairs 56–63. Figure 4 (left panel) shows the scatter plot of UN data x:life expectancy versus y: latitude; note that the true causal direction is  $y \to x$ . We compute the causal parameters by maximizing the log likelihood (4) with  $\lambda = 50$  given the true causal direction  $y \to x$ . The



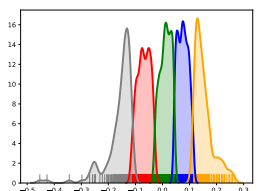


Figure 4: Top panel: the UN life expectancy dataset is clustered to k=5 using our clustering algorithm. Bottom panel: the density plot of the of the causal parameters  $\theta_i$ .

<sup>1</sup>https://webdav.tuebingen.mpg.de/cause-effect/

test statistic without adjustment is 14.90 and its theoretical 5% quantile is 0.60, so it mistakenly rejects the null.

The statistic after adjustment using clustering labels with k = 2, 3, 4 still rejects the true direction but with a larger p-value.

However with k=5 gives aggregated test statistic t=1.73 with the 5% theoretical quantile 2.21, so infers the causal direction correctly. The correct direction is inferred also for  $k\geq 6$ . Our clustering algorithm converges on 7 clusters.

Next we check the performance of our method on all data pairs as well. Following [5] we exclude pairs 12,17, 47, 52, 53, 54, 55, 70, 71, 101, and 105. Additionally we excluded pairs 73, 106, and 68 that include outliers. These outliers yielded singleton clusters and made the computation of cluster specific test statistic numerically unstable.

We sample 90 data from each pair and repeat this process 50 times independently. Then estimate the causal parameters by maximizing the log likelihood (4) with  $\lambda=50$  for  $x\to y$  and  $y\to x$  directions. We choose  $k=K\pm 2$  with a visually appealing  $2\le K\le 6$  for each data set. We used the clustering labels to adjust HSIC statistic while running our clustering algorithm. Figure 5 shows the boxplot of type I error. Theoretically the type I error must remain under control about the significance level. However, the mean of type I error probability for

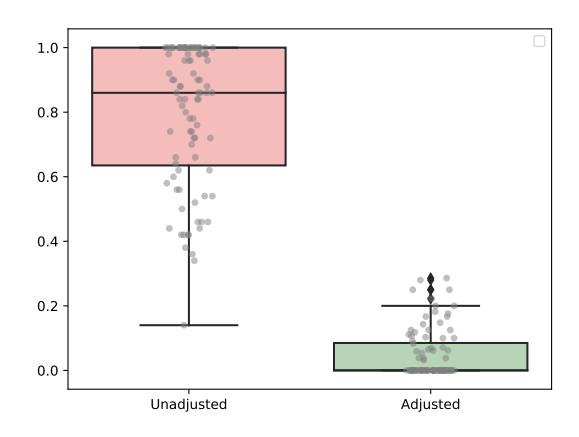


Figure 5: Boxplot of type I error probability of Tüebingen cause-effect pairs without and with adjustment.

unadjusted statistic is 0.796 while the adjusted method it is reaches to 0.048. The the total error probability (type I error + type II error) remain equal.

### 6 Conclusion

In this manuscript, we have developed a probabilistic clustering method that allows clustering causal parameters with flexible number of clusters and derived a deterministic version that resembles k-means. It is well-known that fitting k-means with model selection methods such as BIC scoring [10] over-estimates the number of components. Our scoring is developed for the clustering context, in which k-means falls matches the setting of linear regression: labelling update is equivalent to design matrix estimation, and mean update is equivalent to the coefficient estimation. The marginal posterior scoring becomes BIC scoring of [10] if  $\kappa\tau=1$  and  $n_c=n$ . Our experiments show  $\kappa=\exp\{kn/4\}$  works well in practice.

We use the clustering labels to adjust the test statistic of causal direction for heterogeneous data. It is clear that ignoring the clustering structure introduces significant bias to the test statistic and yields an uncontrolled type I error probability. It is evident that the HSIC test statistic used in causal direction identification heavily rely on single component assumption. It requires proper adjustment using clustering labels in the case of heterogeneous data.

### References

- [1] Arthur Gretton, Olivier Bousquet, Alex Smola, and Bernhard Schölkopf. Measuring statistical dependence with hilbert-schmidt norms. In *International Conference on Algorithmic Learning Theory*, pages 63–77. Springer, 2005.
- [2] Arthur Gretton, Alexander J Smola, Olivier Bousquet, Ralf Herbrich, Andrei Belitski, Mark Augath, Yusuke Murayama, Jon Pauls, Bernhard Schölkopf, and Nikos K Logothetis. Kernel constrained covariance for dependence measurement. In *AISTATS*, volume 10, pages 112–119, 2005.
- [3] John A Hartigan. Partition models. Communications in Statistics Theory and Methods, 19(8):2745–2756, 1990.
- [4] Patrik O Hoyer, Dominik Janzing, Joris M Mooij, Jonas Peters, and Bernhard Schölkopf. Nonlinear causal discovery with additive noise models. In *Advances in Neural Information Processing Systems*, pages 689–696, 2009.

- [5] Shoubo Hu, Zhitang Chen, Vahid Partovi Nia, Laiwan Chan, and Yanhui Geng. Causal inference and mechanism clustering of a mixture of additive noise models. In S. Bengio, H. Wallach, H. Larochelle, K. Grauman, N. Cesa-Bianchi, and R. Garnett, editors, *Advances in Neural Information Processing Systems 31*, pages 5206–5216. 2018.
- [6] Dominik Janzing and Bernhard Scholkopf. Causal inference using the algorithmic markov condition. *IEEE Transactions on Information Theory*, 56(10):5168–5194, 2010.
- [7] Neil Lawrence. Probabilistic non-linear principal component analysis with gaussian process latent variable models. *Journal of Machine Learning Research*, 6(Nov):1783–1816, 2005.
- [8] Furui Liu and Laiwan Chan. Causal discovery on discrete data with extensions to mixture model. *ACM Transactions on Intelligent Systems and Technology (TIST)*, 7(2):21, 2016.
- [9] Joris M Mooij, Jonas Peters, Dominik Janzing, Jakob Zscheischler, and Bernhard Schölkopf. Distinguishing cause from effect using observational data: methods and benchmarks. *The Journal of Machine Learning Research*, 17(1):1103–1204, 2016.
- [10] Dan Pelleg, Andrew W Moore, et al. X-means: Extending k-means with efficient estimation of the number of clusters. In *International Conference on Machine Learning*, volume 1, pages 727–734, 2000.
- [11] Shohei Shimizu, Patrik O Hoyer, Aapo Hyvärinen, and Antti Kerminen. A linear non-gaussian acyclic model for causal discovery. *Journal of Machine Learning Research*, 7(Oct):2003–2030, 2006.
- [12] Andrew TA Wood, James G Booth, and Ronald W Butler. Saddlepoint approximations to the cdf of some statistics with nonnormal limit distributions. *Journal of the American Statistical Association*, 88(422):680–686, 1993.
- [13] Kun Zhang and Aapo Hyvärinen. On the identifiability of the post-nonlinear causal model. In *Conference on Uncertainty in Artificial Intelligence*, pages 647–655. AUAI Press, 2009.

## **Broader Impact**

Many modern artificial intelligence applications involve automatic decision making using a predictive model trained on large data sets. Concrete examples are self-driving cars, drones, automatic biomedical image recognition for various deceases such as cancer, COVID-19, genetic malfunction, etc. Such scenarios all involve heterogeneous data and require cause-and-effect analysis, specially if the decision system malfunctions. Practitioners must be cautious about the data heterogeneity. We showed that the inference about the causal direction is highly sensitive to homogeneous data assumption. We demonstrate how to correct the inference by embedding a clustering method in the test statistic and improve its performance.

### **Appendix**

### **Proof of Theorem 1:**

The proof is by re-arranging the log likelihood terms. The conditional log likelihood of  $\boldsymbol{\theta} \mid \boldsymbol{\mu}$  is  $\ell(\boldsymbol{\mu}) = -\frac{1}{2}\log|2\pi\sigma^2\mathbf{I}| - \frac{1}{2}(\mathbf{Z}\boldsymbol{\theta} - \boldsymbol{\mu})^{\top}(\mathbf{Z}\boldsymbol{\theta} - \boldsymbol{\mu})$  which is a quadratic function of  $\boldsymbol{\mu}$ . We may re-write it using a quadratic Taylor expansion

$$\ell(\boldsymbol{\mu}) = \ell(\hat{\boldsymbol{\mu}}) + \nabla \ell(\boldsymbol{\mu})|_{\boldsymbol{\mu} = \hat{\boldsymbol{\mu}}} (\boldsymbol{\mu} - \hat{\boldsymbol{\mu}}) + \frac{1}{2} (\boldsymbol{\mu} - \hat{\boldsymbol{\mu}})^{\top} \left\{ \nabla^{2} \ell(\boldsymbol{\mu}) \right\}^{-1} (\boldsymbol{\mu} - \hat{\boldsymbol{\mu}})$$

in which  $\ell(\hat{\boldsymbol{\mu}}) = -\frac{N}{2}\log 2\pi\sigma^2 - \frac{1}{2\sigma^2}\sum_{c=1}^k\sum_{\{i|z_i=c\}}(\theta_i - \bar{\theta}_c)^2$ ,  $\nabla\ell(\boldsymbol{\mu}) = \sigma^2\mathbf{Z}^{\top}(\boldsymbol{\theta} - \mathbf{Z}\boldsymbol{\mu})$ ,  $\nabla^2\ell(\boldsymbol{\mu}) = -\sigma^2\mathbf{Z}^{\top}\mathbf{Z}$  and  $\hat{\boldsymbol{\mu}} = [\bar{\theta}_1,\dots,\bar{\theta}_k]$  is the maximum likelihood estimator with  $\nabla\ell(\boldsymbol{\mu})|_{\boldsymbol{\mu}=\hat{\boldsymbol{\mu}}} = 0$ . Therefore

$$\ell(\boldsymbol{\mu}) = \ell(\hat{\boldsymbol{\mu}}) - \frac{1}{2\sigma^2} (\boldsymbol{\mu} - \hat{\boldsymbol{\mu}}) (\mathbf{Z}^{\top} \mathbf{Z})^{-1} (\boldsymbol{\mu} - \hat{\boldsymbol{\mu}}).$$

Hence

$$\exp\{\ell(\mathbf{z}\mid\boldsymbol{\theta})\} = \frac{1}{\sqrt{|2\pi\kappa\tau^{2}\sigma^{2}\mathbf{I}|}} \int \cdots \int \exp\left\{\ell(\boldsymbol{\mu}) - \frac{1}{2\kappa\tau^{2}\sigma^{2}}(\boldsymbol{\mu} - \hat{\boldsymbol{\mu}})^{\top}(\boldsymbol{\mu} - \hat{\boldsymbol{\mu}})\right\} d\boldsymbol{\mu} 
= \frac{\exp\{\ell(\hat{\boldsymbol{\mu}})\}}{(2\pi\kappa\tau^{2}\sigma^{2})^{\frac{k}{2}}} \int \cdots \int \exp\left\{-\frac{1}{2}(\boldsymbol{\mu} - \hat{\boldsymbol{\mu}})^{\top}\left(\frac{1}{\sigma^{2}}\mathbf{Z}^{\top}\mathbf{Z} + \frac{1}{\kappa\tau^{2}\sigma^{2}}\mathbf{I}\right)(\boldsymbol{\mu} - \hat{\boldsymbol{\mu}})\right\} d\boldsymbol{\mu} 
= \frac{\exp\ell(\hat{\boldsymbol{\mu}})\sqrt{\left|2\pi\sigma^{2}\left(\mathbf{Z}^{\top}\mathbf{Z} + \frac{1}{\kappa\tau^{2}}\mathbf{I}\right)^{-1}\right|}}{(2\pi\kappa\tau^{2}\sigma^{2})^{\frac{k}{2}}},$$

but  $\mathbf{Z}^{\top}\mathbf{Z}$  is a diagonal matrix with diagonal elements  $n_c$ , so the latter term simplifies further to

$$\frac{\exp\{\ell(\hat{\boldsymbol{\mu}})\}}{\sqrt{\prod_{c=1}^{k}(n_c\kappa\tau^2+1)}}.$$

and (8) is derved after putting the pieces together

$$\ell(\mathbf{z} \mid \boldsymbol{\theta}) = \ell(\hat{\boldsymbol{\mu}}) - \frac{1}{2} \sum_{c=1}^{k} \log(\kappa \tau^2 n_c + 1).$$

**Proof of Theorem 2:** The proof is a multi-stage Gibbs sampler adaptation for the clustering case with varying cluster components. First we ensure that sampling from the discrete multivariate posterior  $p(\mathbf{z} \mid \boldsymbol{\mu}, \boldsymbol{\theta}, k)$  and continuous multivariate  $p(\boldsymbol{\mu} \mid \mathbf{z}, \boldsymbol{\theta}, k)$  converges to the joint  $p(\boldsymbol{\mu}, \mathbf{z} \mid \boldsymbol{\theta}, k)$ . Note that  $p(\boldsymbol{\mu} \mid \boldsymbol{\theta}, \mathbf{z}, k)$  is multivariate Gaussian and  $p(\mathbf{z} \mid \boldsymbol{\theta}, \boldsymbol{\mu}, k)$  is discrete with support  $\{1, \dots, k\}^N$ . Define the positive Markov transition kernel

$$k(\mathbf{z} \mid \mathbf{z}') = \int \cdots \int p(\mathbf{z} \mid \boldsymbol{\mu}, \boldsymbol{\theta}, k) p(\boldsymbol{\mu} \mid \mathbf{z}', \boldsymbol{\theta}, k) d\boldsymbol{\mu}.$$

This transition kernel is equivalent to taking intermediate samples from  $\mu_t \sim p(\mu \mid \mathbf{z}_{t-1}, \boldsymbol{\theta}, k)$  at iteration t and drawing  $\mathbf{z}_t \sim p(\mathbf{z} \mid \boldsymbol{\mu}_t, \boldsymbol{\theta}, k)$ .

It is easy to check that  $k(\mathbf{z} \mid \mathbf{z}')$  is reversible thus is invariant with respect to the marginal  $p(\mathbf{z} \mid \boldsymbol{\theta}, k)$ .

Now let's sample from the multivariate  $p(\mathbf{z} \mid \boldsymbol{\mu}, \boldsymbol{\theta}, k)$  using univariate multinomial samplers. Suppose  $k_1(\mathbf{z} \mid \mathbf{z}')$  is the transition kernel equivalent to univariate Gibbs sampler of  $p(\mathbf{z} \mid \boldsymbol{\mu}, \boldsymbol{\theta}, k)$  in increasing order  $z_1, \dots, z_N$ , i.e.

$$k_{1}(\mathbf{z} \mid \mathbf{z}') = p(z'_{1} \mid z_{2}, \dots, z_{N}, \boldsymbol{\mu}, \boldsymbol{\theta}, k) p(z'_{2}, \mid z'_{1}, z_{3}, \dots, z_{N}, \boldsymbol{\mu}, \boldsymbol{\theta}, k) \cdots p(z'_{N} \mid z'_{1}, \dots, z'_{N-1}, \boldsymbol{\mu}, \boldsymbol{\theta}, k)$$

$$\sum_{z_{1}, \dots, z_{n}} k_{1}(\mathbf{z} \mid \mathbf{z}') p(\mathbf{z} \mid \boldsymbol{\mu}, \boldsymbol{\theta}, k)$$

$$= \sum_{z_{1}, \dots, z_{n}} p(z'_{1} \mid z_{2}, \dots, z_{N}, \boldsymbol{\mu}, \boldsymbol{\theta}, k) \cdots p(z'_{N} \mid z'_{1}, \dots, z'_{N-1}, \boldsymbol{\mu}, \boldsymbol{\theta}, k)$$

$$p(z_{1} \mid z_{2}, \dots, z_{N}, \boldsymbol{\mu}, \boldsymbol{\theta}, k) p(z_{2}, \dots, z_{N} \mid \boldsymbol{\mu}, \boldsymbol{\theta}, k)$$

$$= \sum_{z_{2}, \dots, z_{n}} p(z'_{2} \mid z'_{1}, \dots, z_{N}, \boldsymbol{\mu}, \boldsymbol{\theta}, k) p(z'_{n} \mid z'_{1}, \dots, z'_{N-1}, \boldsymbol{\mu}, \boldsymbol{\theta}, k) p(z'_{1}, z_{2}, \dots, z_{N})$$

in which we integrated over  $z_1$  and decomposed

$$p(z'_1, z_2, \ldots, z_N \mid \boldsymbol{\mu}, \boldsymbol{\theta}, k) = p(z'_1 \mid z_2, \ldots, z_N, \boldsymbol{\mu}, \boldsymbol{\theta}, k) p(z_2, \ldots, z_N \mid \boldsymbol{\mu}, \boldsymbol{\theta}).$$

Continue by decomposing

$$p(z_1', z_2, \ldots, z_N \mid \boldsymbol{\mu}, \boldsymbol{\theta}, k) = p(z_2 \mid z_1', z_3, \ldots, z_N \mid \boldsymbol{\mu}, \boldsymbol{\theta}, k) p(z_1', z_3, \ldots, z_N \mid \boldsymbol{\mu}, \boldsymbol{\theta}, k)$$

and summing over  $z_2$ . Repeating this re-arranging and summing over  $z_3, \ldots, z_N$  ends up with  $p(z_1', \ldots, z_N' \mid \boldsymbol{\mu}, \boldsymbol{\theta}, k) = p(\mathbf{z}' \mid \boldsymbol{\mu}, \boldsymbol{\theta}, k)$ .

A similar argument applies to  $\mu_t \sim p(\mu \mid \mathbf{z}, \boldsymbol{\theta})$  to replace the intermediate sampler with univariate conditional samplers and to show

$$p(\boldsymbol{\mu}' \mid \mathbf{z}, \boldsymbol{\theta}) = \int \cdots \int k_2(\boldsymbol{\mu} \mid \boldsymbol{\mu}') p(\boldsymbol{\mu} \mid \mathbf{z}, \boldsymbol{\theta}) d\boldsymbol{\mu}$$

in which

$$k_2(\boldsymbol{\mu} \mid \boldsymbol{\mu}') = p(\mu_1' \mid \mu_2, \dots, \mu_c, \mathbf{z}, \boldsymbol{\theta}) p(\mu_2' \mid \mu_1', \mu_3, \dots, \mu_c, \mathbf{z}, \boldsymbol{\theta}) \cdots p(\mu_c' \mid \mu_1', \dots, \mu_{c-1}').$$

Simple posterior calculations show these univariate distributions that construct the kernel  $k_1$  are multinomial  $z_i \sim \mathcal{M}(1, \pi_i)$  with probabilities

$$\boldsymbol{\pi}_i = \left[ \frac{\phi\left(\frac{\theta_i - \mu_1}{\sigma}\right)}{\sum_{c=1}^k \phi\left(\frac{\theta_i - \mu_c}{\sigma}\right)}, \dots, \frac{\phi\left(\frac{\theta_i - \mu_c}{\sigma}\right)}{\sum_{c=1}^k \phi\left(\frac{\theta_i - \mu_c}{\sigma}\right)} \right],$$

and the intermediate univariate samplers are Gaussian with mean  $\bar{\theta}_c(1+\frac{1}{N_c\kappa\tau^2})^{-1}$  and variance  $\sigma^2(N_c+\frac{1}{\kappa\tau^2})^{-1}$ . The label update step has  $k_1$  and the mean update has  $k_2$  transition kernel. Implementing these two steps sequentially is equivalent to a chain with the composition transition kernel  $k_1 \circ k_2$ . The last step is to margin over the cluster components k.

Assume a discrete uniform prior on  $k \in \{K - \Delta, K + \Delta\}$  which allows to define a posterior proportional to the likelihood. Note that k does not affect the dimension of the marginalized posterior  $p(\mathbf{z} \mid \boldsymbol{\theta}, k)$ , otherwise transdimensional samplers need to be developed. Marginalizing over k adds another step to the algorithm and implies sampling  $k \sim \mathcal{M}(1, \pi)$  in which

$$\boldsymbol{\pi} = \begin{bmatrix} \exp\{\ell(\mathbf{z} \mid \boldsymbol{\theta}, k = K - \Delta)\} \\ \frac{K + \Delta}{\sum_{k = K - \Delta}} \exp\{\ell(\mathbf{z} \mid \boldsymbol{\theta}, k)\} & \sum_{k = K - \Delta} \exp\{\ell(\mathbf{z} \mid \boldsymbol{\theta}, k)\} \end{bmatrix}.$$

**Proof of Theorem 3:** The product partition model (5) imposes mutually independent random pairs  $(x_i, y_i)$  across clusters. Therefore, given a certain causal direction their projection  $\theta_i = g(x_i, y_i)$  are independent across clusters too. A similar argument holds for HSIC as a function of  $\theta_i$ . This allows us to use the asymptotic result of the homogeneous case [1] in each sub-population c and combine them based on product partition independence assumption.

For large  $n_c$  inside cluster c

$$n_c \text{HSIC}_c \sim \sum_{l=1}^{\infty} \lambda_l z_l^2 \approx \Gamma(\alpha, \beta)$$

in which  $\lambda_l$  are constants and  $z_l$  are independent standard Gaussian random variables with  $\mu_c = \mathbb{E}(\mathrm{HSIC}_c)$ ,  $\sigma_c^2 = \mathbb{V}(\mathrm{HSIC}_c)$ . Define the aggregated test statistic

$$t = \sum_{c=1}^{k} n_c \text{HSIC}_c = \sum_{c=1}^{k} \sum_{l=1}^{\infty} \lambda_{cl} z_{cl}^2$$

which is clearly another countable sum  $\sum_{m=1}^{\infty} \gamma_m w_m^2$  after swapping the sum order and re-arranging terms m=(l-1)k+c.